

DESY 08-141
 Edinburgh 2009/01
 LTH 819
 January 2009

Non-perturbative improvement of stout-smeared three flavour clover fermions

N. Cundy^a, M. Göckeler^a, R. Horsley^b, T. Kaltenbrunner^a,
 A. D. Kennedy^b, Y. Nakamura^{ac}, H. Perlt^d, D. Pleiter^c,
 P. E. L. Rakow^e, A. Schäfer^a, G. Schierholz^{af}, A. Schiller^d,
 H. Stüben^g and J. M. Zanotti^b

– QCDSF-UKQCD Collaboration –

^a Institut für Theoretische Physik, Universität Regensburg,
 93040 Regensburg, Germany

^b School of Physics and Astronomy, University of Edinburgh,
 Edinburgh EH9 3JZ, UK

^c Deutsches Elektronen-Synchrotron DESY,
 15738 Zeuthen, Germany

^d Institut für Theoretische Physik, Universität Leipzig,
 04109 Leipzig, Germany

^e Theoretical Physics Division, Department of Mathematical Sciences,
 University of Liverpool, Liverpool L69 3BX, UK

^f Deutsches Elektronen-Synchrotron DESY,
 22603 Hamburg, Germany

^g Konrad-Zuse-Zentrum für Informationstechnik Berlin,
 14195 Berlin, Germany

Abstract

We discuss a 3-flavour lattice QCD action with clover improvement in which the fermion matrix has single level stout smearing for the hopping terms together with unsmeared links for the clover term. With the (tree-level) Symanzik improved gluon action this constitutes the **Stout Link Non-perturbative Clover** or SLiNC action. To cancel $O(a)$ terms the clover term coefficient has to be tuned. We present here results of a non-perturbative determination of this coefficient using the Schrödinger functional and as a by-product a determination of the critical hopping parameter. Comparisons of the results are made with lowest order perturbation theory.

1 Introduction and $O(a)$ improvement

When constructing a lattice QCD action, even the simplest gluon action has only $O(a^2)$ corrections. The naive quark action also has $O(a^2)$ corrections, but suffers from the ‘doubling problem’ describing 16 flavours in the continuum limit. A cure is to add the Wilson mass term, so 15 flavours decouple in the continuum limit, but the price is that there are now $O(a)$ corrections (and also loss of chiral invariance), so that for example for a ratio of hadron masses

$$\frac{m_H}{m_{H'}} = r_0 + ar_1 + O(a^2). \quad (1)$$

The Symanzik approach is a systematic improvement to $O(a^n)$ (where in practice $n = 2$ for the fermion action) by adding a basis (an asymptotic series) of irrelevant operators and tuning their coefficients to remove completely $O(a^{n-1})$ effects. Restricting improvement to on-shell quantities the equations of motion reduce the set of operators in both the action and in matrix elements. Indeed, for $O(a)$ improvement of the fermion action only one additional flavour-singlet operator is required

$$\mathcal{L}_{clover} \propto ac_{sw} \sum_{q,x,\mu\nu} \bar{q}(x)\sigma_{\mu\nu}F_{\mu\nu}(x)q(x), \quad (2)$$

the so-called ‘Sheikholeslami–Wohlert’ or ‘clover’ term, [1]. So if we can improve *one* on-shell quantity this then fixes c_{sw} as a function of the lattice spacing a or equivalently of the bare coupling g_0^2 , so that all other on-shell quantities are automatically improved to $O(a)$, i.e., we now have

$$\frac{m_H}{m_{H'}} = r_0 + O(a^2). \quad (3)$$

A non-perturbative determination of c_{sw} will be the main goal of this paper, the general approach being described below.

Matrix elements still require additional $O(a)$ operators, for example for the axial current and pseudoscalar density, [2]¹,

$$\begin{aligned} \mathcal{A}_\mu &= (1 + b_A a m_q)(A_\mu + c_A a \partial_\mu^{LAT} P) \\ \mathcal{P} &= (1 + b_P a m_q)P, \end{aligned} \quad (4)$$

(for mass degenerate quarks) with

$$A_\mu = \bar{q}\gamma_\mu\gamma_5 q, \quad P = \bar{q}\gamma_5 q, \quad (5)$$

¹We implicitly distinguish between quark flavours in operators, i.e. consider non-singlet operators.

which require additional b_A , c_A and b_P improvement coefficients. An easily determined quantity is the quark mass computed from the PCAC WI relation²,

$$m_q^{WI} = \frac{\langle \partial_0^{LAT}(A_0(x_0) + c_A a \partial_0^{LAT} P(x_0)) O \rangle}{2 \langle P(x_0) O \rangle}. \quad (6)$$

Choosing different operators, O , gives different determinations of the quark mass $m_q^{WI(i)}$, $i = 1, 2$ with different lattice artifacts. If the quark mass is improved then its errors are $O(a^2)$. So we can determine the ‘optimal’ c_{sw} improvement coefficient by tuning until

$$m_q^{WI(1)} = m_q^{WI(2)}. \quad (7)$$

(This is equivalent to considering the renormalised quark mass

$$m_{qR} = \frac{Z_A(1 + b_A a m_q)}{Z_P(1 + b_P a m_q)} m_q^{WI}. \quad (8)$$

In general the b_A , b_P coefficients do affect considerations of $O(a)$ -improvement. However, here one imposes a condition at fixed bare parameters (g_0^2, m_q) which means that the factors drop out.) Practically, how this is achieved will be discussed in this paper after the action is introduced.

This paper is organised as follows. In the next section, section 2, the action is given and in the following section the Schrödinger functional is briefly discussed, together with the general procedure for determining the optimal c_{sw} and optimal critical hopping parameter, κ_c . Section 4 gives some lattice details for a series of simulations at various coupling constants, which after suitable interpolations leads to this determination. Section 5 then discusses possible finite size effects in the results. Results are collected together in section 6 and a polynomial interpolation (in the coupling constant) for both c_{sw} and κ_c are given, together with a comparison with the lowest order perturbation result. Finally in section 7 some brief conclusions are discussed. Tables of the raw results are given in appendix A.

2 The SLiNC action

We shall consider here $n_f = 3$ flavour stout link clover fermions – SLiNC fermions (Stout Link Non-perturbative Clover). In a little more detail, for each flavour,

$$\begin{aligned} S_F = & \sum_x \left\{ \kappa \sum_\mu [\bar{q}(x)(\gamma_\mu - 1)\tilde{U}_\mu(x)q(x + a\hat{\mu}) - \bar{q}(x)(\gamma_\mu + 1)\tilde{U}_\mu^\dagger(x - a\hat{\mu})q(x - a\hat{\mu})] \right. \\ & \left. + \bar{q}(x)q(x) - \frac{1}{2}\kappa a c_{sw} \sum_{\mu\nu} \bar{q}(x)\sigma_{\mu\nu} F_{\mu\nu}(x)q(x) \right\}. \end{aligned} \quad (9)$$

² ∂_μ^{LAT} is the symmetric lattice derivative, $(\partial_\mu^{LAT} f)(x) = [f(x + a\hat{\mu}) - f(x - a\hat{\mu})]/(2a)$, and (no μ summation), $(\partial_\mu^{2 LAT} f)(x) = [f(x + a\hat{\mu}) - 2f(x) + f(x - a\hat{\mu})]/a^2 = (\partial_\mu^{LAT} \partial_\mu^{LAT} f)(x) + O(a^2)$.

Rescaling the quark fields $q \rightarrow q/\sqrt{2\kappa}$ gives the quark mass m_q where

$$m_q(c_{sw}) = \frac{1}{2a} \left(\frac{1}{\kappa} - \frac{1}{\kappa_c(c_{sw})} \right), \quad (10)$$

which is proportional to the PCAC quark mass, m_q^{WI} . The loss of chiral invariance means that for a given c_{sw} a critical hopping parameter, $\kappa_c(c_{sw})$ has now also to be determined.

The hopping terms (Dirac kinetic term and Wilson mass term, i.e. those terms involving a κ) in eq. (9) use a once stout smeared link or ‘fat link’, [3],

$$\begin{aligned} \tilde{U}_\mu &= \exp\{iQ_\mu(x)\} U_\mu(x) \\ Q_\mu(x) &= \frac{\alpha}{2i} [VU^\dagger - UV^\dagger - \frac{1}{3}\text{Tr}(VU^\dagger - UV^\dagger)], \end{aligned} \quad (11)$$

(V_μ is the sum of all staples around U_μ) while the clover term remains built from ‘thin’ links – they are already of length $4a$ and we want to avoid the fermion matrix becoming too extended. Smearing is thought to help at present lattice spacings by smoothing out fluctuations in the gauge fields slightly and so reducing the condition number and also to avoid a near first order phase transition. The critical kappa in eq. (10) corresponds to an additive mass renormalisation

$$m_c(c_{sw}) = \frac{1}{2a} \left(\frac{1}{\kappa_c(c_{sw})} - \frac{1}{1/8} \right). \quad (12)$$

It is known that with a combination of link fattening and increase of the clover coefficient, it is possible to reduce this mass term [4, 5, 6]. The stout variation is also analytic which means that the derivative in the gauge group can be taken (so the force in the Hybrid Monte Carlo, or HMC, simulation is well defined) and perturbative expansions are also possible, [7].

To complete the action we also use the Symanzik tree-level gluon action

$$\begin{aligned} S_G = & \quad (13) \\ \frac{6}{g_0^2} \left\{ c_0 \sum_{Plaquette} \frac{1}{3} \text{Re Tr}(1 - U_{Plaquette}) + c_1 \sum_{Rectangle} \frac{1}{3} \text{Re Tr}(1 - U_{Rectangle}) \right\}, \end{aligned}$$

together with

$$c_0 = \frac{20}{12}, \quad c_1 = -\frac{1}{12} \quad \text{and} \quad \beta = \frac{6c_0}{g_0^2} = \frac{10}{g_0^2}. \quad (14)$$

While this gluon action has elements of higher order improvement, namely $O(a^4)$, this is not the reason that it is used here. (The best we can hope for the fermion action is $O(a^2)$ improvement.) Again we wish to move the action away from a nearby first-order phase transition occurring when using the standard Wilson action (i.e. $c_0 \rightarrow 1$, $c_1 \rightarrow 0$), [8] by using a slightly extended action. Different values of c_0 and c_1 can be and have been used in the literature to address this problem, e.g. [8].

3 The Schrödinger functional

The ALPHA Collaboration determined the improvement coefficients by means of the ‘Schrödinger functional’, [9, 10, 11, 2]. Some numerical results for c_{sw} for the quenched case ($n_f = 0$) were given in [12, 13], for $n_f = 2$ flavours in [14] and for $n_f = 3$ flavours in [15, 16, 17]. In this approach Dirichlet boundary conditions are applied on the time boundaries to the fields. For the gluon fields, fixing them on the boundary is then equivalent to inducing some classical background field about which they fluctuate. It is simplest to consider spatially constant colour diagonal fields, corresponding to a constant chromo-electric background field. Concretely, we consider a $L^3 \times T$ lattice (with $T = 2L$) and take the background field to be

$$\begin{aligned} U_0^c(\vec{x}, x_0) &= 1 \\ U_k^c(\vec{x}, x_0) &= \exp\left(-i\frac{a}{T}[x_0 C^{(2)} + (T - x_0) C^{(1)}]\right), \end{aligned} \quad (15)$$

with

$$C^{(i)} = \frac{1}{L} \begin{pmatrix} \phi_1^{(i)} & 0 & 0 \\ 0 & \phi_2^{(i)} & 0 \\ 0 & 0 & \phi_3^{(i)} \end{pmatrix}, \quad (16)$$

and

$$(\phi_1^{(1)}, \phi_2^{(1)}, \phi_3^{(1)}) = (-\frac{1}{6}\pi, 0, \frac{1}{6}\pi), \quad (\phi_1^{(2)}, \phi_2^{(2)}, \phi_3^{(2)}) = (-\frac{5}{6}\pi, \frac{1}{3}\pi, \frac{1}{2}\pi), \quad (17)$$

and fix the boundary values a posteriori. As we have an extended gauge action (rather than the simpler Wilson gluon action), we fix two values at each double boundary layer and so we choose, following [18]³, U_μ^c from eq. (15) at $x_0 = -a$, 0 (lower boundary) and similarly U_μ^c at $x_0 = T - a$ and T (upper boundary). The ‘bulk’ of the lattice is thus from $x_0 = 0$ to $x_0 = T - a$. Additionally the weight factors for the gluon loops in eq. (14) must be appropriately chosen on the boundary for $O(a)$ -improvement. Classically these weight factors are not difficult to find, however a full non-perturbative determination would be difficult. But away from the boundaries, they only affect the local PCAC relation to $O(a^2)$ and so are not essential for the determination of the optimal c_{sw} , and so it is sufficient to use the classical values.

The fixed boundary quark fields, $\rho, \bar{\rho}$ (taken as zero here) make simulations with $m_q \sim 0$ with no zero mode problems possible. They are specified on the lower inner boundary and upper inner boundary from

$$\begin{aligned} P_0^+ q(\vec{x}, 0) &= \rho^{(1)}(\vec{x}) \\ \bar{q}(\vec{x}, 0) P_0^- &= \bar{\rho}^{(1)}(\vec{x}) \\ P_0^- q(\vec{x}, T - a) &= \rho^{(2)}(\vec{x}) \\ \bar{q}(\vec{x}, T - a) P_0^+ &= \bar{\rho}^{(2)}(\vec{x}), \end{aligned} \quad (18)$$

³An alternative procedure using single layer boundaries is given in [19].

where P_0^\pm is the projection operator defined by

$$P_0^\pm = \frac{1}{2} (1 \pm \gamma_0) . \quad (19)$$

These projections are necessary for consistency. $\rho, \bar{\rho}$ can be taken as sinks and sources respectively to build operators for correlation functions. For example here we can take at the lower inner boundary $x_0 = 0$ ($i = 1$) and upper inner boundary $x_0 = T - a$ ($i = 2$) the operators

$$O^{(i)} = \sum_{\vec{y}, \vec{z}} \left(-\frac{\delta}{\delta \rho^{(i)}(\vec{y})} \right) \gamma_5 \left(\frac{\delta}{\delta \bar{\rho}^{(i)}(\vec{z})} \right) . \quad (20)$$

So we can investigate PCAC behaviour at different distances from the boundaries.

In a little more detail, following eq. (6), we first set

$$r^{(i)}(x_0) = \frac{\partial_0^{LAT} f_A^{(i)}(x_0)}{2f_P^{(i)}(x_0)}, \quad s^{(i)}(x_0) = a \frac{\partial_0^{2LAT} f_P^{(i)}(x_0)}{2f_P^{(i)}(x_0)}, \quad (21)$$

where

$$\begin{aligned} f_A^{(1)}(x_0) &= -\frac{1}{n_f^2 - 1} \langle A_0(x_0) O^{(1)} \rangle \\ f_A^{(2)}(T - x_0) &= +\frac{1}{n_f^2 - 1} \langle A_0(x_0) O^{(2)} \rangle, \end{aligned} \quad (22)$$

and

$$\begin{aligned} f_P^{(1)}(x_0) &= -\frac{1}{n_f^2 - 1} \langle P(x_0) O^{(1)} \rangle \\ f_P^{(2)}(T - x_0) &= -\frac{1}{n_f^2 - 1} \langle P(x_0) O^{(2)} \rangle. \end{aligned} \quad (23)$$

Then redefine the quark mass slightly, but which coincides to $O(a^2)$ for the improved theory

$$M^{(i)}(x_0, y_0) = r^{(i)}(x_0) + \hat{c}_A(y_0) s^{(i)}(x_0), \quad \hat{c}_A(y_0) = -\frac{r^{(1)}(y_0) - r^{(2)}(y_0)}{s^{(1)}(y_0) - s^{(2)}(y_0)}, \quad (24)$$

which eliminates the unknown c_A in the determination of the quark mass, [12] and replaces it by an estimator, \hat{c}_A . Improvement is defined when

$$(M, \Delta M) = (0, 0), \quad (25)$$

where

$$M \equiv M^{(1)}, \quad \Delta M \equiv M^{(1)} - M^{(2)}, \quad (26)$$

are chosen at some suitable x_0 , [12]. This gives the required optimal c_{sw} and κ_c , which we will denote by a star: c_{sw}^* and κ_c^* . Conventionally, we choose

$$M \equiv M^{(1)}(T/2, T/4), \quad \Delta M \equiv M^{(1)}(3T/4, T/4) - M^{(2)}(3T/4, T/4). \quad (27)$$

There are small changes due to the finite volume used, so eq. (25) becomes

$$(M, \Delta M) = (0, \Delta M^{tree}), \quad (28)$$

where ΔM^{tree} is the tree-level (i.e. $g_0^2 = 0$, $c_{sw} \equiv c_{sw}^{tree} = 1$) value of $\Delta M|_{M=0}$ on the $L^3 \times T$ lattice. This ensures that $c_{sw} \rightarrow 1$ exactly as $\beta \rightarrow \infty$. For $\alpha = 0$, the analytic result on a $N_s^3 \times 2N_s = 8^3 \times 16$ lattice (where $L = aN_s$) is 0.000277, [12]. Carrying out the interpolation procedures outlined in the next section for a free configuration, with background field given by eq. (15) yields 0.000271. For the stout smearing used here (see next section) we find this is reduced to $\Delta M^{tree} = 0.000066$ and so we have neglected ΔM^{tree} in the following and simply used eq. (25).

4 The lattice simulation

The 3-flavour lattice simulation used the Chroma software library, [20], the Schrödinger functional details following [18]. Results were mostly generated on $N_s^3 \times 2N_s \equiv 8^3 \times 16$ lattices, together with some additional $12^3 \times 24$ lattices, using the HMC algorithm together with the RHMC variation, [21], for the 1-flavour. A mild smearing of $\alpha = 0.1$ was used. A series of simulations were performed (typically generating $O(3000)$ trajectories for the $8^3 \times 16$ lattices and $O(2000)$ trajectories for the $12^3 \times 24$ lattices), quadratic and then linear interpolations of the $(M, \Delta M)$ results being used to locate the optimal point, $(0, 0)$ as described below. Some further details and tables of the results are given in appendix A. (Preliminary results were given in [22].)

4.1 c_{sw}^*

We have a two-parameter interpolation in c_{sw} and κ which is split here into two separate interpolations. First plotting ΔM against M and then interpolating to $M = 0$ for fixed c_{sw} gives a critical κ namely $\kappa_c(c_{sw})$,

$$\Delta M(c_{sw}, \kappa)|_{M=0} \equiv \Delta M(c_{sw}, \kappa_c(c_{sw}))|_{M=0} \equiv \Delta M(c_{sw}). \quad (29)$$

In Figs. 1, 2 we plot ΔM versus M for various c_{sw} values for the $8^3 \times 16$ lattices and in Fig. 3 the results for the $12^3 \times 24$ lattices.

These graphs are the fundamental plots requiring high statistics as ΔM is the difference between two different M s. As there are always 4 (or more) points for

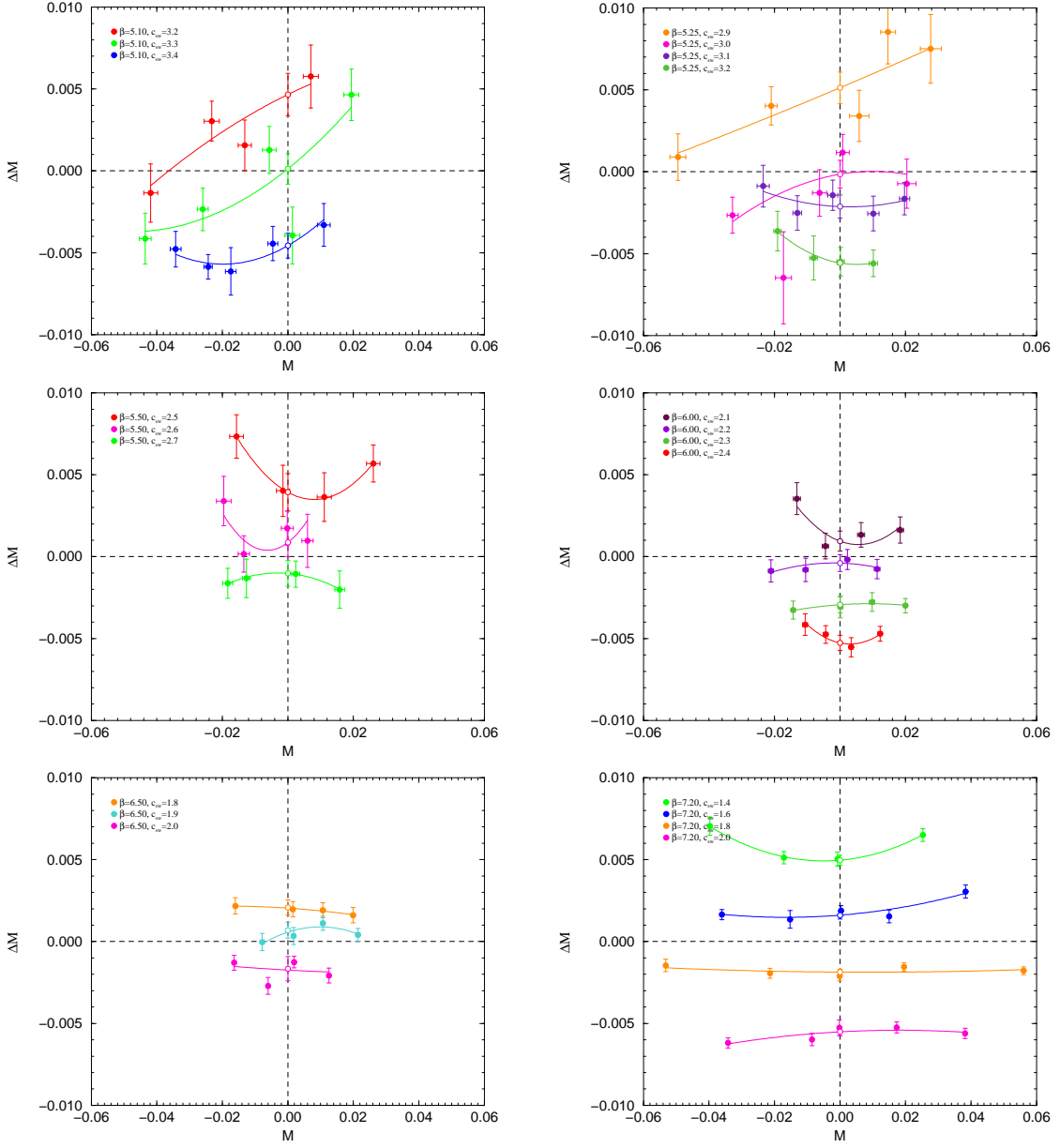


Figure 1: ΔM against M for $\beta = 5.10, 5.25$ (upper left, right pictures respectively) for $\beta = 5.50, \beta = 6.00$ (middle left, right pictures respectively), and for $\beta = 6.50, \beta = 7.20$ (lower left, right pictures respectively), together with quadratic interpolations to $M = 0$ (the open symbols).

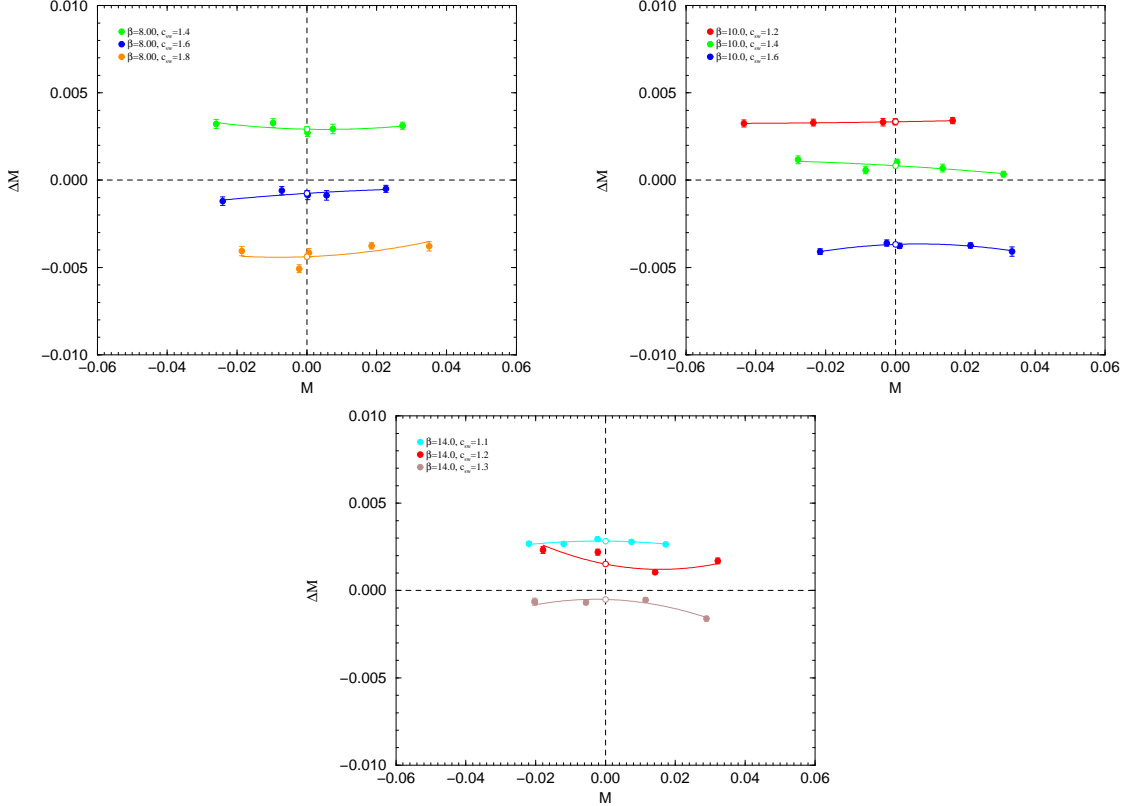


Figure 2: ΔM against M for $\beta = 8.00, 10.0$ (upper left, right pictures respectively) and for $\beta = 14.0$, (lower picture), together with quadratic interpolations to $M = 0$ (the open symbols).

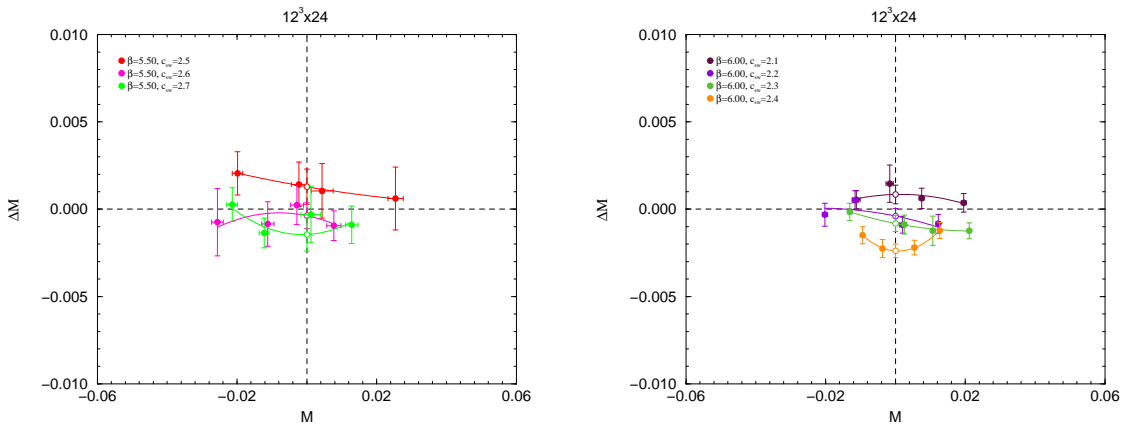


Figure 3: ΔM against M for $\beta = 5.50, 6.00$ (left, right pictures respectively) on a $12^3 \times 24$ lattice together with quadratic interpolations to $M = 0$ (the open symbols).

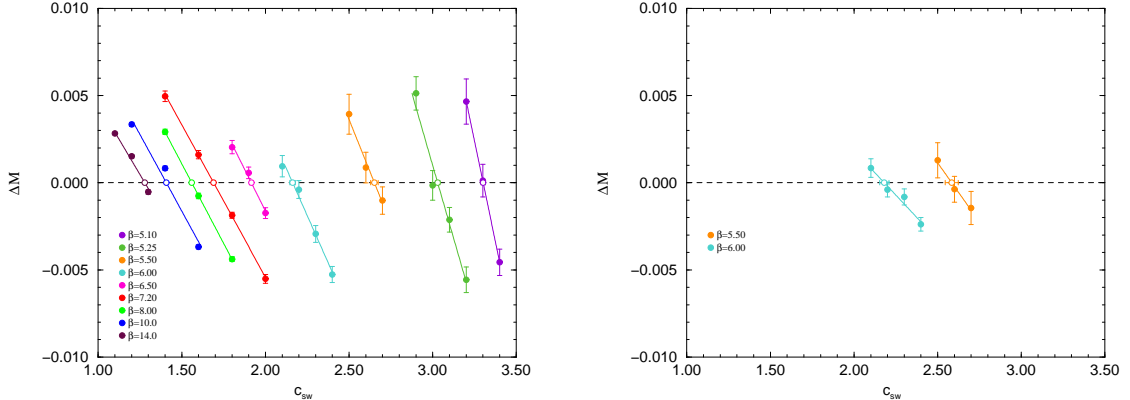


Figure 4: ΔM at $M = 0$ against c_{sw} for various values of β (filled circles) together with linear interpolations to $\Delta M = 0$ (open circles). The left plot shows the $8^3 \times 16$ results while the right plot shows the $12^3 \times 24$ results.

each graph a quadratic fit is made and the value of ΔM is determined where M vanishes.

These values of $\Delta M(c_{sw})$ for each β value are then plotted against c_{sw} as shown in Fig. 4 together with linear fits. The point where $\Delta M(c_{sw})$ vanishes gives c_{sw}^* . This gives values of

$$c_{sw}^* = \left\{ \begin{array}{ll} 3.302(13) & \beta = 5.10 \\ 3.030(13) & \beta = 5.25 \\ 2.651(23) & \beta = 5.50 \\ 2.163(17) & \beta = 6.00 \\ 1.915(10) & \beta = 6.50 \\ 1.690(07) & \beta = 7.20 \\ 1.559(05) & \beta = 8.00 \\ 1.407(04) & \beta = 10.0 \\ 1.279(06) & \beta = 14.0 \end{array} \right\}_{8^3 \times 16} \quad (30)$$

$$\left. \begin{array}{ll} 2.584(38) & \beta = 5.50 \\ 2.181(28) & \beta = 6.00 \end{array} \right\}_{12^3 \times 24}$$

We postpone a discussion of possible finite size effects until section 5.

From Fig. 4, we see that linear fits even for four points (the $\beta = 7.20, 6.00, 5.25$ results) show very little curvature, so that we may write, [14]

$$\Delta M(c_{sw}) = \omega(c_{sw} - c_{sw}^*), \quad (31)$$

with the gradient, ω , a slowly varying function of g_0 . To test this we note that

$$\frac{\partial \Delta M(c_{sw})}{\partial c_{sw}} = \omega, \quad (32)$$

so a fit to the gradients in Fig. 4 (for the $8^3 \times 16$ lattices) yields an estimate for ω . We find that ω is constant with an approximate value of -0.018 , although for the largest values of g_0^2 there are deviations from this.

4.2 κ_c^*

A similar procedure yields κ_c^* : plotting M against $1/\kappa$ and interpolating quadratically to $M = 0$ for fixed c_{sw} gives the critical κ , denoted by $\kappa_c(c_{sw})$. Then subsequently plotting $\Delta M(c_{sw})$ against $1/\kappa_c(c_{sw})$ and interpolating using a linear fit to $\Delta M = 0$ gives κ_c^* .

We first plot M against $1/\kappa$ for the $8^3 \times 16$ results in Figs. 5, 6 and for the $12^3 \times 24$ results in Fig. 7.

Note that to produce these graphs should not require high statistics as it does not involve ΔM . (Although these are not the fundamental graphs they are also useful in helping to determine the various (c_{sw}, κ) values for the runs.)

These $\Delta M(\kappa_c)$ are then plotted in Fig. 8 again with a linear fit. Where ΔM vanishes gives κ_c^* . For legibility the results have been split into sub-graphs. We see that κ_c^* is a non-monotonic function of β .

We find results of

$$\kappa_c^* = \left\{ \begin{array}{ll} 0.116227(180) & \beta = 5.10 \\ 0.118385(184) & \beta = 5.25 \\ 0.121125(330) & \beta = 5.50 \\ 0.124043(199) & \beta = 6.00 \\ 0.124825(107) & \beta = 6.50 \\ 0.125343(61) & \beta = 7.20 \\ 0.125281(38) & \beta = 8.00 \\ 0.124993(22) & \beta = 10.0 \\ 0.124773(26) & \beta = 14.0 \end{array} \right\}_{8^3 \times 16} \quad (33)$$

$$\left. \begin{array}{ll} 0.122086(554) & \beta = 5.50 \\ 0.123849(330) & \beta = 6.00 \end{array} \right\}_{12^3 \times 24}$$

As a consistency check the alternative plot of c_{sw} against $1/\kappa_c$ is shown in Fig. 9 where c_{sw} is plotted against $1/\kappa_c(c_{sw})$, again with a linear fit between the points. The optimal values of c_{sw} , namely c_{sw}^* , taken from the previous fits as given in eq. (30) are shown as dashed horizontal lines, the intersection with the $1/\kappa_c$ curves then giving the optimal critical values of κ_c , namely κ_c^* . These are denoted in the figure as open points. As a comparison, the results from the previous determination of κ_c^* , eq. (33), are also shown as vertical lines. We see good agreement between the different determinations of κ_c^* , which indicates that the fit procedure adopted here gives consistent results for both c_{sw}^* and κ_c^* .

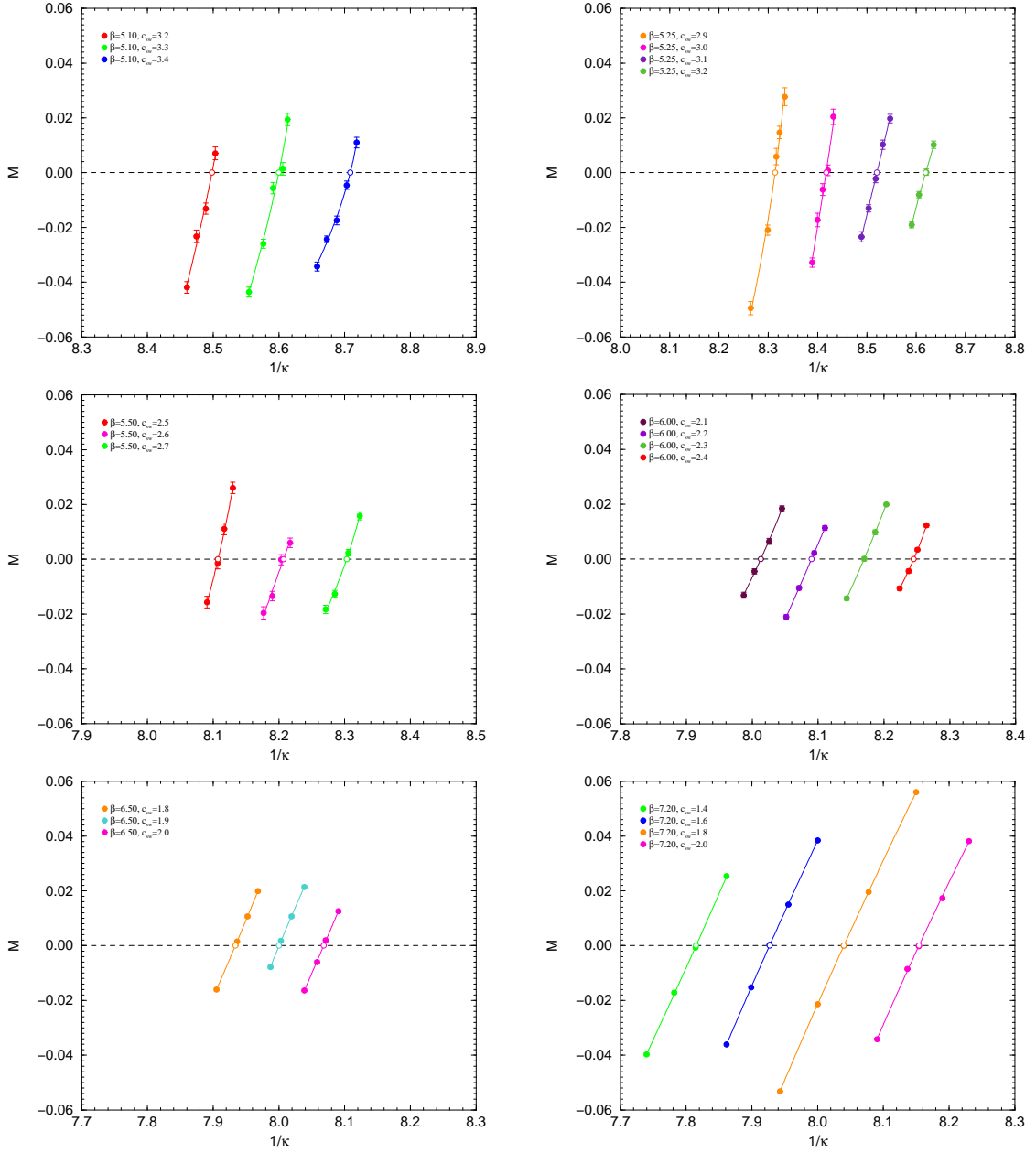


Figure 5: M against $1/\kappa$ for $\beta = 5.10, 5.25$ (upper left, right pictures respectively) for $\beta = 5.50$, $\beta = 6.00$ (middle left, right pictures respectively), and for $\beta = 6.50, \beta = 7.20$ (lower left, right pictures respectively), together with quadratic interpolations to $M = 0$ (the open symbols).

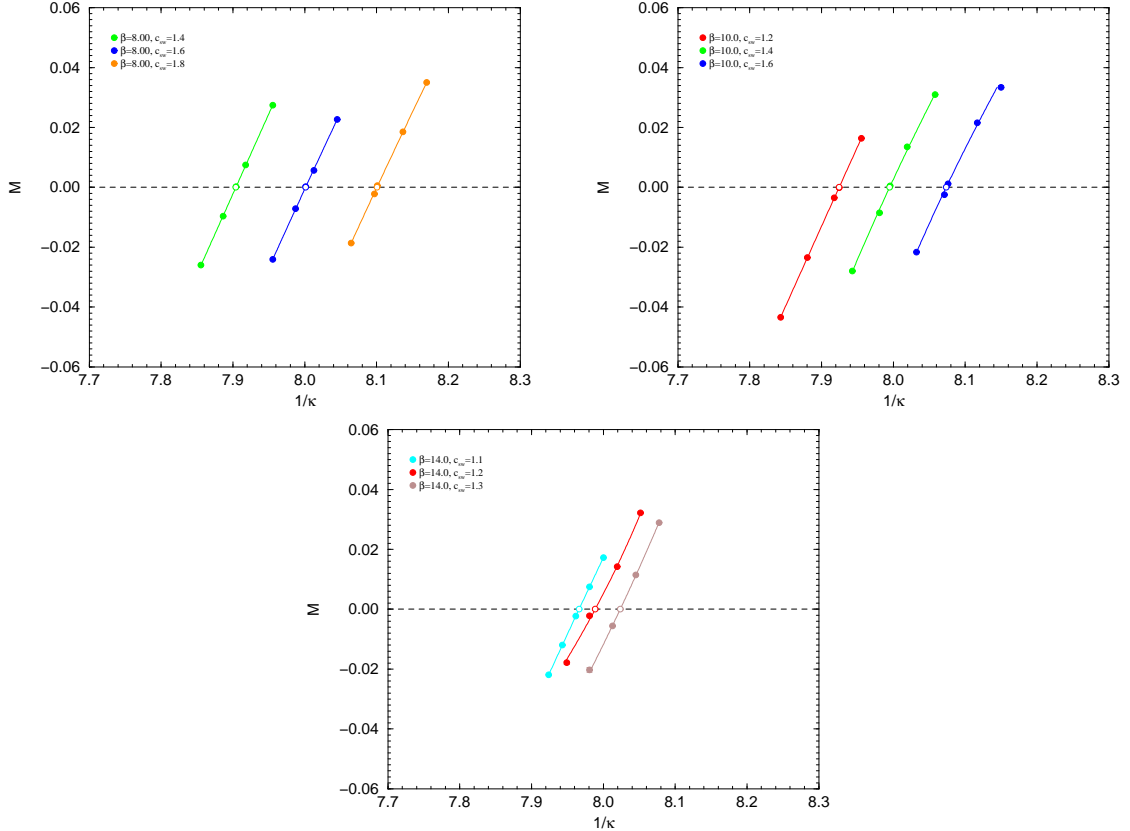


Figure 6: M against $1/\kappa$ for $\beta = 8.00, 10.0$ (upper left, right pictures respectively) and for $\beta = 14.0$, (lower picture), together with quadratic interpolations to $M = 0$ (the open symbols).

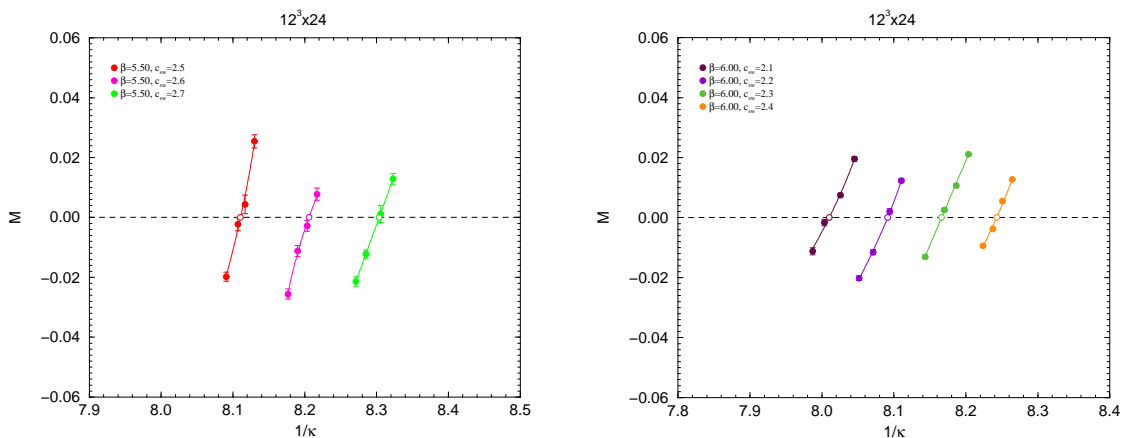


Figure 7: M against $1/\kappa$ for $\beta = 5.50, 6.00$ (left, right pictures respectively) on a $12^3 \times 24$ lattice together with quadratic interpolations to $M = 0$ (the open symbols).

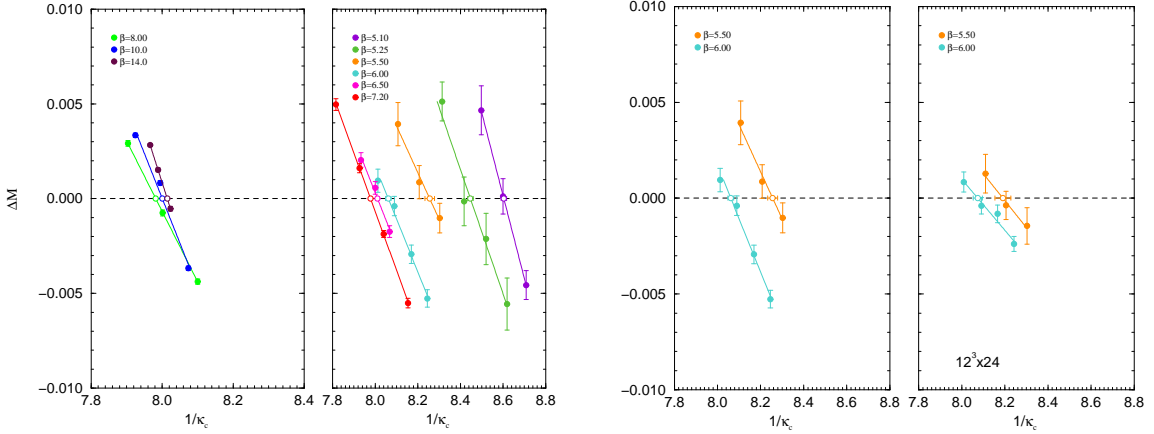


Figure 8: Results of $\Delta M(\kappa_c(c_{sw}))$ versus $1/\kappa_c$ together with linear fits. The open circles give the optimal critical κ_c s, i.e. the κ_c^* s. The two left plots show the $8^3 \times 16$ results while the two right plots compare the $\beta = 5.50, 6.00$ $8^3 \times 16$ results with the $12^3 \times 24$

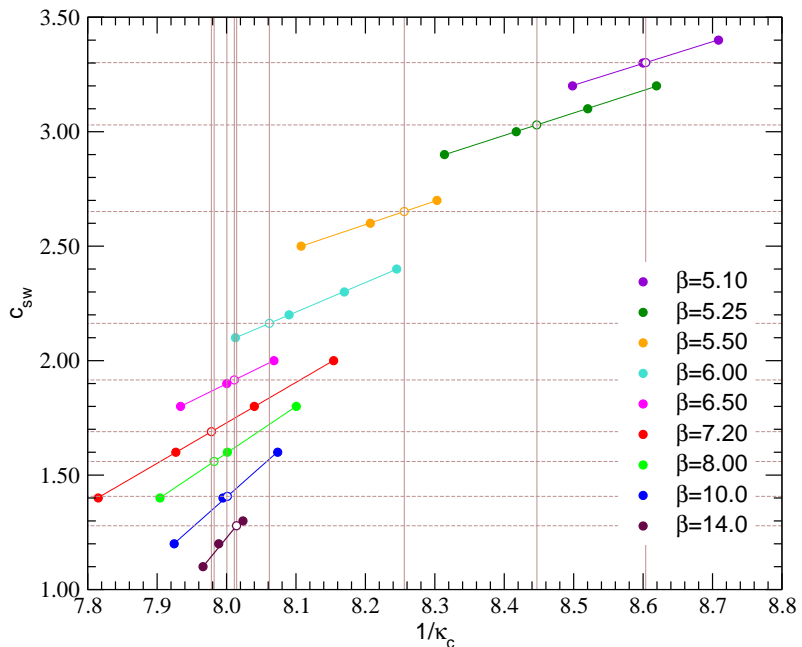


Figure 9: Results of c_{sw} (filled circles) versus $1/\kappa_c$ together with linear fits. The optimal c_{sw} , c_{sw}^* , from eq. (30) are shown as dashed horizontal lines. The open circles are the intersection of the linear fits with these horizontal lines and give an alternative determination of the optimal critical κ_c , κ_c^* , which are to be compared with the results of eq. (33) shown as vertical lines.

Finally note that plotting the $n_f = 2$ flavour results would yield a similar curve to Fig. 9.

For future reference (in section 6.2) as the fits in Fig. 9 are all linear then we write

$$\frac{1}{\kappa_c} = \frac{1}{\kappa_c^*} + d(c_{sw} - c_{sw}^*) , \quad (34)$$

with a measured coefficient $d(g_0)$,

$$d = \left\{ \begin{array}{ll} 1.0521(92) & \beta = 5.10 \\ 1.0208(54) & \beta = 5.25 \\ 0.9783(100) & \beta = 5.50 \\ 0.7753(53) & \beta = 6.00 \\ 0.6722(51) & \beta = 6.50 \\ 0.5658(11) & \beta = 7.20 \\ 0.4907(10) & \beta = 8.00 \\ 0.3719(08) & \beta = 10.0 \\ 0.2704(23) & \beta = 14.0 \end{array} \right\} 8^3 \times 16 \quad (35)$$

5 Finite size effects

There are (small) ambiguities due to the finite volume used. In an infinite volume we expect $O(a\Lambda_{QCD})$ contributions (in the chiral limit, otherwise there are also extra $O(am_q)$ terms) due to the different boundary conditions or operators chosen. In a finite volume there are additional $O(a/L)$ terms. Thus might expect asymptotically, following [16],

$$c_{sw}^*(g_0, L/a) = c_{sw}^*(g_0, \infty) + c_L \frac{a}{L} + c_\Lambda a\Lambda_{QCD} + \dots . \quad (36)$$

The terms proportional to $a\Lambda_{QCD}$ vanish as a (or g_0^2) $\rightarrow 0$ and represent the ambiguities in the different definitions of M . For a physical quantity \mathcal{Q} , then

$$\begin{aligned} \mathcal{Q} &= \mathcal{Q}(a) + q_L (c_{sw}^*(g_0, L/a) - c_{sw}^*(g_0, \infty)) a\Lambda_{QCD} + O(a^2) \\ &= \mathcal{Q}(a) + q_L c_L \frac{a}{L} a\Lambda_{QCD} + O(a^2) . \end{aligned} \quad (37)$$

The correction term may be re-written as (where $L = aN_s$)

$$q_L c_L \frac{a}{L} a\Lambda_{QCD} = \frac{q_L c_L}{N_s} a\Lambda_{QCD} . \quad (38)$$

Potentially this might mean that \mathcal{Q} is no longer $O(a)$ improved for simulations where c_{sw}^* has been determined on a fixed lattice size, N_s . However it is likely that the unknown coefficients q_L and c_L are small and coupled with the N_s factor in the denominator, this is then expected to be a small effect.

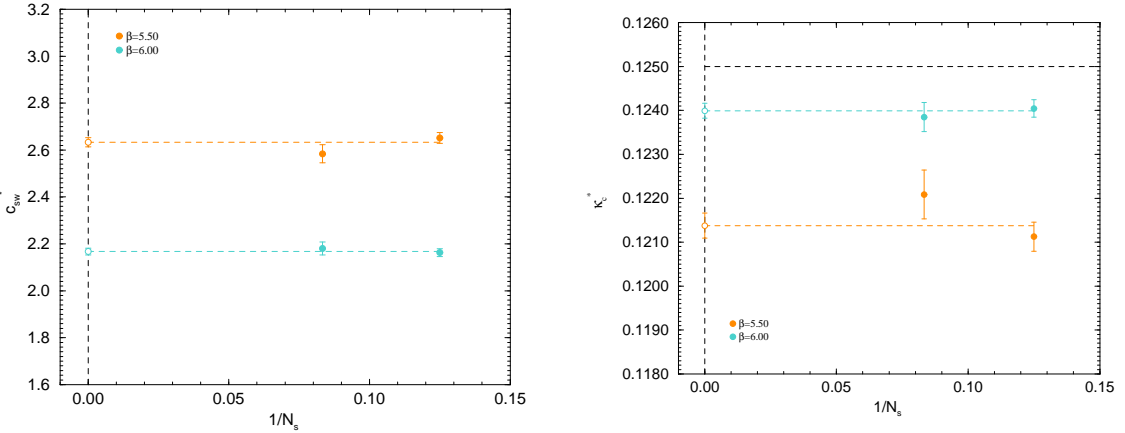


Figure 10: c_{sw}^* against $1/N_s$ (left picture) and κ_c^* against $1/N_s$ (right picture) for $\beta = 5.50, 6.00$, filled circles. Also shown are constant fits (dashed lines) together with the extrapolated values (open circles).

To avoid this altogether we can either keep L fixed in physical units as $a \rightarrow 0$ (the ‘constant physics condition’) so $O(a/L) \rightarrow 0$, or alternatively simulate for several values of N_s and extrapolate to $N_s \rightarrow \infty$. The ‘Poor man’s solution’ is to evaluate at large $\beta \rightarrow \infty$ (i.e. on a free configuration for $N_s = 8$ here) and subtract this result. Practically, following the same procedure as in section 4.1 we have found that for c_{sw} this $O(1/N_s)$ term (for $N_s = 8$) is negligible.

As noted previously we have also performed additional simulations on larger lattices $12^3 \times 24$ for $\beta = 6.00, 5.50$ in order to discuss finite lattice size corrections. The results are plotted in Figs. 3, 7 and compared with the $8^3 \times 16$ results in Figs. 4, 8. At tree level we have, [23],

$$\Delta M^{tree} = k (c_{sw}^{tree} - 1) \frac{a}{L} + \dots, \quad (39)$$

which would indicate that for larger N_s then ΔM becomes smaller, with the consequent noise/signal ratio becoming worse. Indeed this is seen in our results, with the $12^3 \times 24$ data being more bunched together in Fig. 3 than for the corresponding $8^3 \times 16$ data in Fig. 1. This may be mitigated somewhat by choosing a larger range of c_{sw} due to the linear nature of the data as seen in Fig. 4 and eq. (31). For $\beta = 6.00$ we have increased the number of c_{sw} s used in the analysis.

In Fig. 10 we plot c_{sw}^* and κ_c^* against $1/N_s$. For both $\beta = 6.00$ and 5.50 there seems to be small finite size effects for c_{sw}^* . For κ_c^* this is also the case for $\beta = 6.00$, while for $\beta = 5.50$ the situation is perhaps a little less clear-cut. However there is no systematic trend in the data and a constant fit always lies within the error bars of the data. So although we cannot come to a definite conclusion, there do not seem to be large finite volume effects, i.e. c_L appears to be small in eq. (36). So in eq. (37) we only expect small violations of $O(a)$ improvement. We shall, in future, just consider the $8^3 \times 16$ data.

6 Results for c_{sw}^* and κ_c^*

6.1 Perturbative results for c_{sw}^* and κ_c^*

Before giving the non-perturbative results for c_{sw}^* and κ_c^* we first recapitulate the perturbative results. The lowest order perturbative limit has been computed for both c_{sw}^* and κ_c^* , [7]. For c_{sw}^* we have

$$c_{sw}^*(g_0) = 1 + (0.196244 + 1.151888\alpha - 4.2391365\alpha^2)g_0^2, \quad (40)$$

where α is the stout smearing parameter, set equal to 0.1 here. This gives

$$c_{sw}^*(g_0) = 1 + c_1 g_0^2, \quad c_1 = 0.269041, \quad (41)$$

i.e. the smearing parameter has increased the value of c_{sw}^* (for $\alpha = 0$, we have $c_1 = 0.196244$). For $\kappa_c(c_{sw}, g_0)$ we have

$$\begin{aligned} \kappa_c(c_{sw}, g_0) = & \frac{1}{8} \left[1 + \left(0.0853699 - 0.961525\alpha + 3.55806\alpha^2 \right. \right. \\ & \left. \left. - (0.025221 - 0.0787379\alpha)c_{sw} - 0.00984224c_{sw}^2 \right) g_0^2 \right], \end{aligned} \quad (42)$$

giving for $\alpha = 0.1$

$$\kappa_c(c_{sw}, g_0) = \frac{1}{8} \left[1 + \left(0.024798 - 0.0173472c_{sw} - 0.00984224c_{sw}^2 \right) g_0^2 \right], \quad (43)$$

and finally for $c_{sw} = c_{sw}^{tree} = 1$,

$$\kappa_c^*(g_0) = \frac{1}{8} \left[1 + k_1 g_0^2 \right], \quad k_1 = -0.002391. \quad (44)$$

(Note that the result for $\kappa_c(c_{sw}, g_0)$ is more general than the one given in [7] when only the result for $c_{sw} = 1$ was given.)

6.2 Non-perturbative results for c_{sw}^* and κ_c^*

The results for c_{sw}^* and κ_c^* against g_0^2 are plotted in Figs. 11, 12 respectively in the range $\beta \geq 5.10$. The lowest order perturbative limits are also shown, eqs. (41) and (44).

An interpolation between the numerically determined points is also shown. For both c_{sw}^* and κ_c^* a 5th order polynomial in g_0^2 proved sufficient. (These interpolation functions are constrained to reproduce the perturbative results, in the $\beta \rightarrow \infty$ limit and therefore, they have four free parameters.) For $c_{sw}^*(g_0)$ we write

$$c_{sw}^*(g_0) = 1 + c_1 g_0^2 + c_2 g_0^4 + c_3 g_0^6 + c_4 g_0^8 + c_5 g_0^{10}, \quad (45)$$

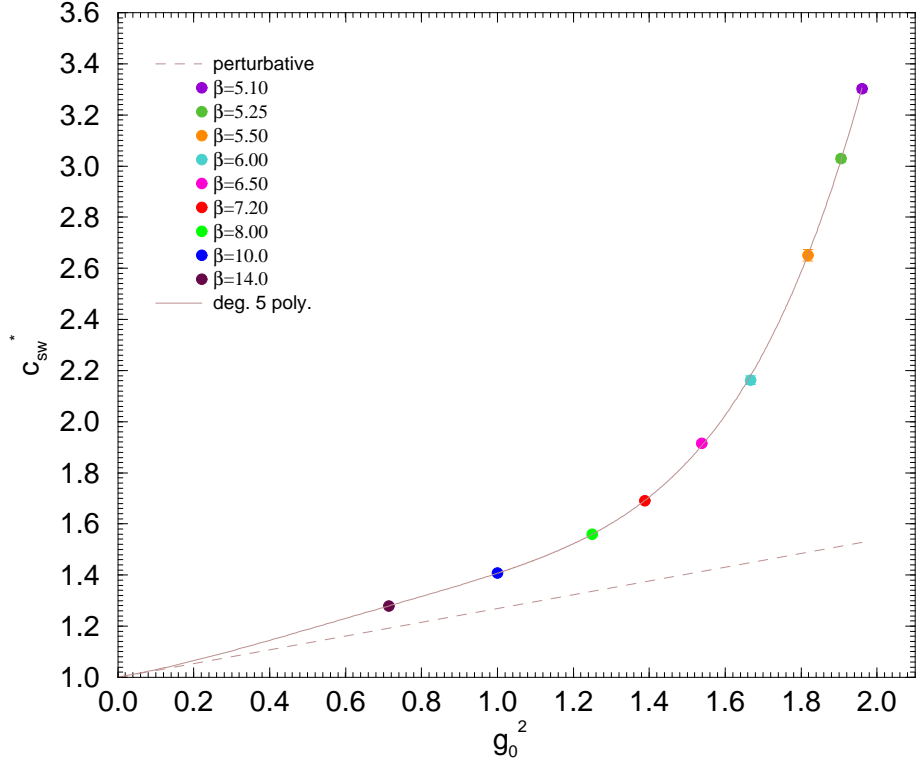


Figure 11: c_{sw}^* against g_0^2 for various values of β (circles), together with a polynomial interpolation (line). Also shown is the perturbative result.

and find

$$\begin{array}{c|c} c_2 & +0.29910 \\ c_3 & -0.11491 \\ c_4 & -0.20003 \\ c_5 & +0.15359 \end{array} \quad (46)$$

while for $\kappa_c^*(g_0)$ we write

$$\kappa_c^*(g_0) = \frac{1}{8} [1 + k_1 g_0^2 + k_2 g_0^4 + k_3 g_0^6 + k_4 g_0^8 + k_5 g_0^{10}], \quad (47)$$

and find

$$\begin{array}{c|c} k_2 & +0.0122470 \\ k_3 & -0.0525676 \\ k_4 & +0.0668197 \\ k_5 & -0.0242800 \end{array} \quad (48)$$

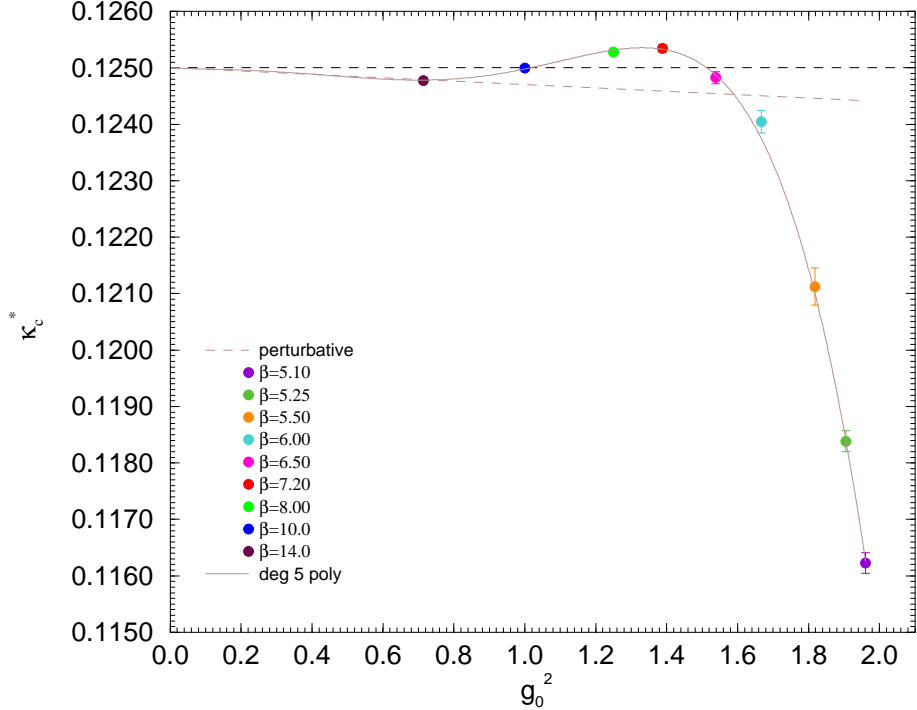


Figure 12: κ_c^* against g_0^2 for various values of β (circles), together with a polynomial interpolation (line). Also shown is the perturbative result.

These give for the specific β values used here

$$c_{sw}^* = \begin{cases} 3.306 & \beta = 5.10 \\ 3.021 & \beta = 5.25 \\ 2.653 & \beta = 5.50 \\ 2.179 & \beta = 6.00 \\ 1.907 & \beta = 6.50 \\ 1.692 & \beta = 7.20 \\ 1.560 & \beta = 8.00 \\ 1.407 & \beta = 10.0 \\ 1.279 & \beta = 14.0 \end{cases} \quad \kappa_c^* = \begin{cases} 0.116262 & \beta = 5.10 \\ 0.118424 & \beta = 5.25 \\ 0.120996 & \beta = 5.50 \\ 0.123751 & \beta = 6.00 \\ 0.124870 & \beta = 6.50 \\ 0.125328 & \beta = 7.20 \\ 0.125314 & \beta = 8.00 \\ 0.124979 & \beta = 10.0 \\ 0.124783 & \beta = 14.0 \end{cases} \quad (49)$$

which are to be compared with the numerically determined values. The errors for c_{sw}^* from the fit are estimated to be about 0.4% while for κ_c^* we have 0.02% at $\beta = 14.0$ rising to 0.15% at $\beta = 5.10$.

These smooth fits between the points give estimates for c_{sw}^* (and κ_c^*) which could be used in the action for future generation of configurations.

For c_{sw}^* the polynomial only tracks the perturbative solution for small values of g_0^2 . This is perhaps not surprising as the tadpole improved, TI , estimate is $c_{sw}^{TI} = u_0^{(S)}/u_0^4$, [7], which is to be compared with the unsmeared case of $c_{sw}^{TI} = 1/u_0^3$

where u_0 is the average plaquette value and $u_0^{(S)}$ is the smeared value. As smearing increases the plaquette value this indicates that c_{sw}^* can be large. For κ_c^* on the other hand as $\kappa_c^{\text{PI}} = 1/(8u_0^{(S)})$ we expect that it is $\sim 1/8$. This is true for reasonably fine lattices, however κ_c^* does begin to decrease for larger values of g_0^2 . For $n_f = 2$ the same phenomenon occurs: for larger g_0^2 , κ_c^* begins to decrease (after initially increasing).

As a further consistency check on the results, we can investigate the gradient $\partial(1/\kappa_c)/\partial c_{sw}|_{c_{sw}^*}$. From eq. (34) we have

$$\left. \frac{\partial(1/\kappa_c)}{\partial c_{sw}} \right|_{c_{sw}^*} = d, \quad (50)$$

as the fits in Fig. 9 are linear, where d is given in eq. (35). Perturbatively we have from eq. (43),

$$\left. \frac{\partial(1/\kappa_c)}{\partial c_{sw}} \right|_{c_{sw}^*} = 8 [0.037032 + 0.019684(c_{sw} - 1)] g_0^2. \quad (51)$$

As g_0 increases c_{sw} increases, so not only do more terms in this expansion become important, but the coefficient of the leading term increases as well. For $c_{sw} = c_{sw}^{\text{tree}} = 1$ we have the leading order perturbative result,

$$\left. \frac{\partial(1/\kappa_c)}{\partial c_{sw}} \right|_{c_{sw}^*} = d_1 g_0^2, \quad d_1 = 0.296253. \quad (52)$$

In Fig. 13 we plot $\partial(1/\kappa_c)/\partial c_{sw}|_{c_{sw}^*}$ against g_0^2 , together with a 5th order polynomial in g_0^2 ,

$$\left. \frac{\partial(1/\kappa_c)}{\partial c_{sw}} \right|_{c_{sw}^*} = d_1 g_0^2 + d_2 g_0^4 + d_3 g_0^6 + d_4 g_0^8 + d_5 g_0^{10}, \quad (53)$$

and find

$$\begin{array}{c|c} d_2 & +0.4180 \\ d_3 & -0.7232 \\ d_4 & +0.4739 \\ d_5 & -0.0919 \end{array} \quad (54)$$

The results follow a smooth curve.

7 Conclusions and Discussion

Non-perturbative $O(a)$ improvement is a viable procedure for (stout) smeared actions with typical clover results being obtained. (Other recent results for 3 flavours are given in [15, 16, 17].) Using the Schrödinger functional method

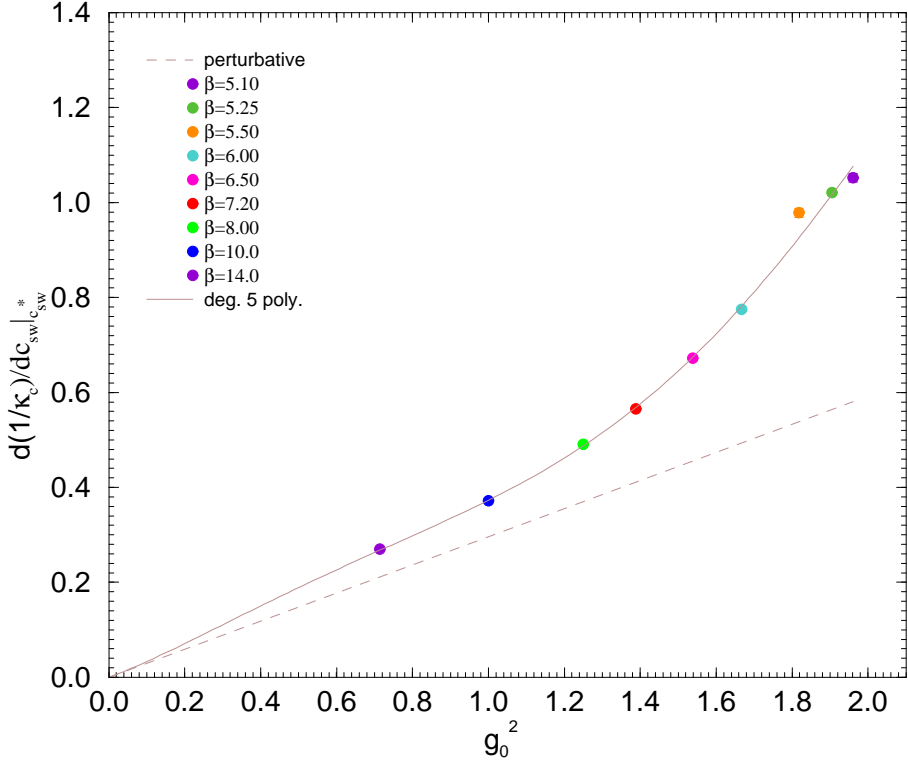


Figure 13: $\partial(1/\kappa_c)/\partial c_{sw}|_{c_{sw}^*}$ against g_0^2 for various values of β (circles), together with a polynomial interpolation (line). Also shown is the perturbative result.

we have determined the optimal clover coefficient, c_{sw}^* necessary to achieve $O(a)$ improvement and also the optimal critical hopping parameter, κ_c^* , eqs. (45), (47) over a wide range of coupling constant.

As a increases we need a significant $c_{sw} \gg c_{sw}^{tree} \equiv 1$ for $O(a)$ improvement. We are now seeking a region where $a \sim 0.05 - 0.1$ fm. Improvement, which is presumably represented by an asymptotic series, brings an advantage for smaller a say $a \leq 0.1$ fm. The two extremes for a are simulations at small a with ‘large’ m_{ps} when there is no continuum extrapolation but a chiral extrapolation, or alternatively simulations at ‘coarse’ a with $m_{ps} \sim m_\pi$ when there is no chiral extrapolation but a continuum extrapolation. Of course the Schrödinger functional does not tell us a ; for this conventional HMC simulations are required. Some preliminary results indicate that around $\beta \sim 5.50$ we have $a \sim 0.08$ fm.

Acknowledgements

The numerical calculations have been performed on the BlueGeneLs at EPCC (Edinburgh, UK), NIC (Jülich, Germany), the QCDOC (Edinburgh, UK) and the

SGI ICE at HLRN (Berlin-Hannover, Germany). We thank all institutions for their support. The Chroma software library was used, [20], and we are grateful to R. G. Edwards and B. Joó for their help and advice. The BlueGene and QC-DOC codes were optimised using BAGEL, [24]. This work has been supported in part by the EU Integrated Infrastructure Initiative Hadron Physics (I3HP) under contract RII3-CT-2004-506078, by the DFG under contracts FOR 465 (Forschergruppe Gitter-Hadronen-Phänomenologie) and SFB/TR 55 (Hadron Physics from Lattice QCD) and the HPC-EUROPA++ project (project number 211437), funded by the European Community’s Research Infrastructure Action within the FP7 “Coordination and support action” Programme. JMZ acknowledges support from STFC Grant PP/F009658/1.

Appendix

A M and ΔM results

We collect here in Tables 1, 2, 3, 4, 5, 6, 7, 8 and 9 the numerical values of M , ΔM as defined in eq. (27) for the $N_s^3 \times 2N_s = 8^3 \times 16$ lattices, while in tables 10 and 11 the results for the $12^3 \times 24$ lattices are given.

The data sets are of size $O(3000)$ trajectories for the $8^3 \times 16$ lattices and $O(2000)$ trajectories for the $12^3 \times 24$ lattices. An initial thermalisation phase was typically of order 300 trajectories. The trajectory length τ_{chroma} was always 1, while the number of steps in the trajectory, $n_{\tau_{chroma}}$, varied for the $8^3 \times 16$ lattices from 10 for $\beta \geq 6.50$ to 12, 12, 15, 18 for $\beta = 6.00, 5.50, 5.25, 5.10$ respectively. This maintained an acceptance rate of $> 80\%$. (This decreased very slightly for the larger β -values.) For the $12^3 \times 24$ lattices $n_{\tau_{chroma}} = 18, 22$ for $\beta = 6.00, 5.50$ was used to give this acceptance.

The jackknife errors for the ratios are given uniformly to two significant figures, with the overriding requirement that the result must also have a minimum of four significant figures. To reduce possible autocorrelations in the data every second trajectory was used with a jackknife block size of 10.

β	c_{sw}	κ	M	ΔM
5.10	3.20	0.11760	0.007049(2313)	0.005762(1923)
5.10	3.20	0.11780	-0.01315(205)	0.001565(1545)
5.10	3.20	0.11800	-0.02324(231)	0.003037(1212)
5.10	3.20	0.11820	-0.04187(212)	-0.001353(1782)
5.10	3.30	0.11610	0.01941(227)	0.004648(1570)
5.10	3.30	0.11620	0.001408(2298)	-0.003942(1737)
5.10	3.30	0.11640	-0.005654(2058)	0.001279(1438)
5.10	3.30	0.11660	-0.02596(166)	-0.002347(1310)
5.10	3.30	0.11690	-0.04356(181)	-0.004137(1550)
5.10	3.40	0.11470	0.01098(191)	-0.003299(1305)
5.10	3.40	0.11490	-0.004606(1516)	-0.004438(1044)
5.10	3.40	0.11510	-0.01742(160)	-0.006135(1442)
5.10	3.40	0.11530	-0.02432(125)	-0.005855(748)
5.10	3.40	0.11550	-0.03424(165)	-0.004780(1086)

Table 1: $8^3 \times 16$ results for M and ΔM for $\beta = 5.10$.

β	c_{sw}	κ	M	ΔM
5.25	2.90	0.12000	0.02772(322)	0.007506(2096)
	2.90	0.12015	0.01468(226)	0.008527(1944)
	2.90	0.12025	0.005850(2967)	0.003412(1559)
	2.90	0.12050	-0.02097(186)	0.004020(1167)
	2.90	0.12100	-0.04947(241)	0.0008952(14184)
5.25	3.00	0.11860	0.02041(279)	-0.0007319(14965)
	3.00	0.11875	0.0008556(19694)	0.001173(1115)
	3.00	0.11890	-0.006210(2160)	-0.001295(1424)
	3.00	0.11905	-0.01727(244)	-0.006479(2808)
	3.00	0.11920	-0.03280(169)	-0.002655(1102)
5.25	3.10	0.11700	0.01973(153)	-0.001642(991)
	3.10	0.11720	0.01021(171)	-0.002551(1054)
	3.10	0.11740	-0.002194(1506)	-0.001440(922)
	3.10	0.11760	-0.01303(133)	-0.002512(1050)
	3.10	0.11780	-0.02344(186)	-0.0008732(12753)
5.25	3.20	0.11580	0.01019(131)	-0.005591(815)
	3.20	0.11600	0.0001673(11516)	-0.005485(875)
	3.20	0.11620	-0.008058(1185)	-0.005259(1342)
	3.20	0.11640	-0.01905(114)	-0.003621(1214)

Table 2: $8^3 \times 16$ results for M and ΔM for $\beta = 5.25$.

β	c_{sw}	κ	M	ΔM
5.50	2.50	0.12300	0.02608(208)	0.005685(1134)
	2.50	0.12320	0.01112(215)	0.003630(1484)
	2.50	0.12335	-0.001449(2014)	0.004018(1567)
	2.50	0.12360	-0.01565(210)	0.007337(1321)
5.50	2.60	0.12170	0.006007(1703)	0.0009700(16220)
	2.60	0.12190	-0.0001614(18320)	0.001739(1046)
	2.60	0.12210	-0.01343(170)	0.0001628(11051)
	2.60	0.12230	-0.01959(223)	0.003397(1508)
5.50	2.70	0.12015	0.01584(149)	-0.002008(1139)
	2.70	0.12040	0.002419(1200)	-0.001062(798)
	2.70	0.12070	-0.01264(125)	-0.001321(1175)
	2.70	0.12090	-0.01831(150)	-0.001626(915)

Table 3: $8^3 \times 16$ results for M and ΔM for $\beta = 5.50$.

β	c_{sw}	κ	M	ΔM
6.00	2.10	0.12430	0.01841(99)	0.001623(800)
	2.10	0.12460	0.006443(1084)	0.001332(753)
	2.10	0.12495	-0.004446(970)	0.0006452(7878)
	2.10	0.12520	-0.01316(107)	0.003539(970)
6.00	2.20	0.12330	0.01135(86)	-0.0007576(5905)
	2.20	0.12355	0.002234(706)	-0.0001747(6084)
	2.20	0.12390	-0.01050(79)	-0.0008061(7138)
	2.20	0.12420	-0.02108(79)	-0.0008650(6771)
6.00	2.30	0.12190	0.01996(58)	-0.002989(439)
	2.30	0.12215	0.009817(838)	-0.002765(574)
	2.30	0.12240	0.0001335(7744)	-0.003061(672)
	2.30	0.12280	-0.01430(67)	-0.003268(549)
6.00	2.40	0.12100	0.01228(69)	-0.004705(456)
	2.40	0.12120	0.003415(610)	-0.005526(586)
	2.40	0.12140	-0.004357(723)	-0.004751(540)
	2.40	0.12160	-0.01066(73)	-0.004149(657)

Table 4: $8^3 \times 16$ results for M and ΔM for $\beta = 6.00$.

β	c_{sw}	κ	M	ΔM
6.50	1.80	0.12550	0.01994(59)	0.001612(472)
	1.80	0.12575	0.01067(59)	0.001914(457)
	1.80	0.12600	0.001513(513)	0.001973(466)
	1.80	0.12650	-0.01600(55)	0.002172(496)
6.50	1.90	0.12440	0.02139(60)	0.0004039(4011)
	1.90	0.12470	0.01068(56)	0.001113(435)
	1.90	0.12495	0.001754(539)	0.0003388(5215)
	1.90	0.12520	-0.007849(601)	-0.00003026(52328)
6.50	2.00	0.12360	0.01255(49)	-0.002074(450)
	2.00	0.12390	0.001931(525)	-0.001253(358)
	2.00	0.12410	-0.006006(505)	-0.002711(510)
	2.00	0.12440	-0.01635(49)	-0.001294(453)

Table 5: $8^3 \times 16$ results for M and ΔM for $\beta = 6.50$.

β	c_{sw}	κ	M	ΔM
7.20	1.40	0.12720	0.02534(46)	0.006503(387)
7.20	1.40	0.12797	-0.0007597(4109)	0.005029(430)
7.20	1.40	0.12850	-0.01713(48)	0.005118(372)
7.20	1.40	0.12920	-0.03970(53)	0.007053(563)
7.20	1.60	0.12500	0.03839(43)	0.003053(391)
7.20	1.60	0.12570	0.01500(38)	0.001534(389)
7.20	1.60	0.12615	0.0003391(4484)	0.001883(311)
7.20	1.60	0.12660	-0.01525(36)	0.001353(543)
7.20	1.60	0.12720	-0.03608(38)	0.001644(307)
7.20	1.80	0.12270	0.05607(29)	-0.001786(239)
7.20	1.80	0.12380	0.01959(32)	-0.001553(260)
7.20	1.80	0.12438	-0.00008070(34186)	-0.002103(288)
7.20	1.80	0.12500	-0.02136(34)	-0.001939(300)
7.20	1.80	0.12590	-0.05319(35)	-0.001455(388)
7.20	2.00	0.12150	0.03819(31)	-0.005604(315)
7.20	2.00	0.12210	0.01736(38)	-0.005245(340)
7.20	2.00	0.12264	-0.0002027(3196)	-0.005262(470)
7.20	2.00	0.12290	-0.008518(356)	-0.005990(375)
7.20	2.00	0.12360	-0.03421(34)	-0.006188(311)

Table 6: $8^3 \times 16$ results for M and ΔM for $\beta = 7.20$.

β	c_{sw}	κ	M	ΔM
8.00	1.40	0.12570	0.02742(25)	0.003117(207)
8.00	1.40	0.12630	0.007469(239)	0.002932(272)
8.00	1.40	0.12651	0.0001971(2329)	0.002716(221)
8.00	1.40	0.12680	-0.009671(223)	0.003270(247)
8.00	1.40	0.12730	-0.02596(28)	0.003221(256)
8.00	1.60	0.12430	0.02266(23)	-0.0004972(2019)
8.00	1.60	0.12480	0.005679(245)	-0.0008718(2676)
8.00	1.60	0.12498	0.0002484(2335)	-0.0008608(2491)
8.00	1.60	0.12520	-0.007169(242)	-0.0006004(2378)
8.00	1.60	0.12570	-0.02410(25)	-0.001201(239)
8.00	1.80	0.12240	0.03501(24)	-0.003785(264)
8.00	1.80	0.12290	0.01858(26)	-0.003763(179)
8.00	1.80	0.12344	0.0005959(2472)	-0.004154(247)
8.00	1.80	0.12350	-0.002196(264)	-0.005071(223)
8.00	1.80	0.12400	-0.01861(27)	-0.004060(270)

Table 7: $8^3 \times 16$ results for M and ΔM for $\beta = 8.00$.

β	c_{sw}	κ	M	ΔM
10.00	1.20	0.12570	0.01641(22)	0.003409(179)
10.00	1.20	0.12619	-0.0001306(1605)	0.003338(182)
10.00	1.20	0.12630	-0.003541(173)	0.003321(217)
10.00	1.20	0.12690	-0.02350(20)	0.003296(198)
10.00	1.20	0.12750	-0.04340(17)	0.003247(206)
10.00	1.40	0.12410	0.03094(21)	0.0003442(1695)
10.00	1.40	0.12470	0.01351(29)	0.0006860(2239)
10.00	1.40	0.12507	0.0004563(4134)	0.001032(171)
10.00	1.40	0.12530	-0.008549(319)	0.0005683(2022)
10.00	1.40	0.12590	-0.02794(27)	0.001172(222)
10.00	1.60	0.12270	0.03342(46)	-0.004086(267)
10.00	1.60	0.12320	0.02152(16)	-0.003744(145)
10.00	1.60	0.12382	0.001171(165)	-0.003759(157)
10.00	1.60	0.12390	-0.002455(294)	-0.003601(186)
10.00	1.60	0.12450	-0.02161(19)	-0.004090(163)

Table 8: $8^3 \times 16$ results for M and ΔM for $\beta = 10.00$.

β	c_{sw}	κ	M	ΔM
14.00	1.10	0.12500	0.01723(8)	0.002646(110)
14.00	1.10	0.12530	0.007452(89)	0.002787(103)
14.00	1.10	0.12560	-0.002273(87)	0.002941(114)
14.00	1.10	0.12590	-0.01196(9)	0.002676(100)
14.00	1.10	0.12620	-0.02194(9)	0.002684(113)
14.00	1.20	0.12420	0.03218(36)	0.001696(167)
14.00	1.20	0.12470	0.01423(16)	0.001044(98)
14.00	1.20	0.12530	-0.002225(329)	0.002191(174)
14.00	1.20	0.12580	-0.01786(46)	0.002320(199)
14.00	1.30	0.12380	0.02900(34)	-0.001514(170)
14.00	1.30	0.12430	0.01132(40)	-0.0004894(1641)
14.00	1.30	0.12480	-0.005572(301)	-0.0007392(1529)
14.00	1.30	0.12530	-0.02027(107)	-0.0009807(2838)

Table 9: $8^3 \times 16$ results for M and ΔM for $\beta = 14.00$.

β	c_{sw}	κ	M	ΔM
5.50	2.50	0.12300	0.02540(221)	0.0006153(17988)
	2.50	0.12320	0.004367(3139)	0.001051(1568)
	2.50	0.12335	-0.002279(2162)	0.001425(1272)
	2.50	0.12360	-0.01981(151)	0.002050(1237)
5.50	2.60	0.12170	0.007744(2026)	-0.0009438(8558)
	2.60	0.12190	-0.002810(1805)	0.0002407(11134)
	2.60	0.12210	-0.01117(179)	-0.0008471(12790)
	2.60	0.12230	-0.02560(168)	-0.0007416(19293)
5.50	2.70	0.12015	0.01289(175)	-0.0008967(10745)
	2.70	0.12040	0.001170(2838)	-0.0003062(16169)
	2.70	0.12070	-0.01224(140)	-0.001362(852)
	2.70	0.12090	-0.02138(153)	0.0002677(9645)

Table 10: $12^3 \times 24$ results for M and ΔM for $\beta = 5.50$.

β	c_{sw}	κ	M	ΔM
6.00	2.10	0.12430	0.01957(74)	0.0003629(5316)
	2.10	0.12460	0.007496(680)	0.0006202(5838)
	2.10	0.12495	-0.001642(1038)	0.001463(1070)
	2.10	0.12520	-0.01123(113)	0.0005411(5241)
6.00	2.20	0.12330	0.01228(67)	-0.0008308(5383)
	2.20	0.12355	0.002046(917)	-0.0008953(4855)
	2.20	0.12390	-0.01153(83)	0.0005139(5375)
	2.20	0.12420	-0.02019(76)	-0.0003129(6525)
6.00	2.30	0.12190	0.02111(49)	-0.001234(455)
	2.30	0.12215	0.01067(68)	-0.001233(833)
	2.30	0.12240	0.002555(557)	-0.0008735(5407)
	2.30	0.12280	-0.01306(64)	-0.0001565(5009)
6.00	2.40	0.12100	0.01273(49)	-0.001217(461)
	2.40	0.12120	0.005458(635)	-0.002194(415)
	2.40	0.12140	-0.003718(533)	-0.002257(514)
	2.40	0.12160	-0.009398(475)	-0.001493(486)

Table 11: $12^3 \times 24$ results for M and ΔM for $\beta = 6.00$.

References

- [1] B. Sheikholeslami and R. Wohlert, *Nucl. Phys.* **B259** (1985) 572.
- [2] M. Lüscher, S. Sint, R. Sommer and P. Weisz, *Nucl. Phys.* **B478** (1996) 365 [[arXiv:hep-lat/9605038](#)].
- [3] C. Morningstar and M. J. Peardon, *Phys. Rev.* **D69** (2004) 054501 [[arXiv:hep-lat/0311018](#)].
- [4] S. Capitani, S. Dürr and C. Hoelbling, *JHEP* **11** (2006) 028 [[arXiv:hep-lat/0607006](#)].
- [5] T. A. DeGrand, A. Hasenfratz and T. G. Kovács, *Nucl. Phys.* **B547** (1999) 259, [[arXiv:hep-lat/9810061](#)].
- [6] S. Boinepalli, W. Kamleh, D. B. Leinweber, A. G. Williams and J. M. Zanotti, *Phys. Lett.* **B616** (2005) 196, [[arXiv:hep-lat/0405026](#)].
- [7] R. Horsley, H. Perlt, P. E. L. Rakow, G. Schierholz and A. Schiller, QCDSF Collaboration, *Phys. Rev.* **D78** (2008) 054504 [[arXiv:0807.0345](#)]; R. Horsley, H. Perlt, P. E. L. Rakow, G. Schierholz and A. Schiller, QCDSF Collaboration, Proceedings of Science PoS(LATTICE 2008)164, [[arXiv:0809.4769 \[hep-lat\]](#)].
- [8] S. Aoki, M. Fukugita, S. Hashimoto, K-I. Ishikawa, N. Ishizuka, Y. Iwasaki, K. Kanaya, T. Kaneko, Y. Kuramashi, M. Okawa, N. Tsutsui, A. Ukawa, N. Yamada and T. Yoshié, JLQCD Collaboration, *Phys. Rev.* **D72** (2005) 054510 [[arXiv:hep-lat/0409016](#)].
- [9] M. Lüscher, R. Narayanan, P. Weisz and U. Wolff, *Nucl. Phys.* **B384** (1992) 168 [[arXiv:hep-lat/9207009](#)].
- [10] S. Sint, *Nucl. Phys.* **B421** (1994) 135 [[arXiv:hep-lat/9312079](#)].
- [11] S. Sint, *Nucl. Phys.* **B451** (1995) 416 [[arXiv:hep-lat/9504005](#)].
- [12] M. Lüscher, S. Sint, R. Sommer, P. Weisz and U. Wolff, *Nucl. Phys.* **B491** (1997) 323 [[arXiv:hep-lat/9609035](#)].
- [13] R. G. Edwards, U. M. Heller and T. R. Klassen, *Phys. Rev. Lett.* **80** (1998) 3448 [[arXiv:hep-lat/9711052](#)].
- [14] K. Jansen and R. Sommer, *Nucl. Phys.* **B530** (1998) 185; Erratum-ibid. **B643** (2002) 517 [[arXiv:hep-lat/9803017](#)].

- [15] N. Yamada, S. Aoki, M. Fukugita, S. Hashimoto, K-I. Ishikawa, N. Ishizuka, Y. Iwasaki, K. Kanaya, T. Kaneko, Y. Kuramashi, M. Okawa, Y. Taniguchi, N. Tsutsui, A. Ukawa and T. Yoshié, CP-PACS, JLQCD Collaborations, *Phys. Rev.* **D71** (2005) 054505 [[arXiv:hep-lat/0406028](https://arxiv.org/abs/hep-lat/0406028)].
- [16] S. Aoki, M. Fukugita, S. Hashimoto, K-I. Ishikawa, N. Ishizuka, Y. Iwasaki, K. Kanaya, T. Kaneko, Y. Kuramashi, M. Okawa, S. Takeda, Y. Taniguchi, N. Tsutsui, A. Ukawa, N. Yamada and T. Yoshié, CP-PACS, JLQCD Collaborations, *Phys. Rev.* **D73** (2006) 034501 [[arXiv:hep-lat/0508031](https://arxiv.org/abs/hep-lat/0508031)].
- [17] R. G. Edwards, B. Joó and H.-W. Lin, *Phys. Rev.* **D78** (2008) 054501 [[arXiv:0803.3960 \[hep-lat\]](https://arxiv.org/abs/0803.3960)].
- [18] T. Klassen, *Nucl. Phys.* **B509** (1998) 391 [[arXiv:hep-lat/9705025](https://arxiv.org/abs/hep-lat/9705025)].
- [19] S. Aoki, R. Frezzotti and P. Weisz, *Nucl. Phys.* **B540** (1999) 501 [[arXiv:hep-lat/9808007](https://arxiv.org/abs/hep-lat/9808007)].
- [20] R. G. Edwards and B. Joó, *Nucl. Phys. Proc. Suppl.* **140** (2005) 832 [[arXiv:hep-lat/0409003](https://arxiv.org/abs/hep-lat/0409003)].
- [21] M. A. Clark and A. D. Kennedy, *Phys. Rev. Lett.* **98** (2007) 051601 [[arXiv:hep-lat/0608015](https://arxiv.org/abs/hep-lat/0608015)].
- [22] N. Cundy, M. Göckeler, R. Horsley, T. Kaltenbrunner, A. D. Kennedy, Y. Nakamura, H. Perlt, D. Pleiter, P. E. L. Rakow, A. Schäfer, G. Schierholz, A. Schiller, H. Stüben, and J. M. Zanotti, QCDSF–UKQCD Collaborations, Proceedings of Science PoS(LATTICE 2008)132, [[arXiv:0811.2355 \[hep-lat\]](https://arxiv.org/abs/0811.2355)].
- [23] M. Lüscher and P. Weisz, *Nucl. Phys.* **B479** (1996) 429 [[arXiv:hep-lat/9606016](https://arxiv.org/abs/hep-lat/9606016)].
- [24] P. A. Boyle, <http://www.ph.ed.ac.uk/~paboyle/bagel/Bagel.html> (2005).